



Original Research Article

Drying Kinetics in Solar Dehydration of Tomato

Rosa A. Olmos-Cruz¹, Guillermo Martínez-Rodríguez^{*1}, Evangelina Sánchez-García²

¹Department of Chemical Engineering, University of Guanajuato, Guanajuato 36050, Mexico

e-mail: ra.olmoscruz@ugto.mx, guimarod@ugto.mx

²Department of Pharmacy, University of Guanajuato, Guanajuato 36050, Mexico

e-mail: evasang@ugto.mx

Cite as: Olmos-Cruz, R. A., Martínez-Rodríguez, G., Sánchez-García, E., Drying Kinetics in Solar Dehydration of Tomato, *J.sustain. dev. energy water environ. syst.*, 13(4), 1130611, 2025,
DOI: <https://doi.org/10.13044/j.sdewes.d13.0611>

ABSTRACT

Of Mexican households, 44.6% reported some degree of food insecurity in 2023. 39.3% of annual tomato production is lost in the supply chain, even though it is among the top staples of the basic food basket. Solar drying tomatoes is a solution for their preservation. A thermodynamic study of four environmental variables was conducted to maximise the kinetics of solar drying of tomatoes during four seasons in 2024. Behaviours of ambient temperature, relative humidity, wind speed, and irradiance were analysed by comparing their boxplot diagrams. Results of the statistical analysis were evaluated in drying kinetics. Relative humidity significantly modifies the kinetics and has a greater impact than irradiance, with a reduction in maximum (15.8 h) and minimum drying times (9.6 h) of up to 40%, and diffusion coefficients and efficiency were maximised by up to 32.1%. Characterising drying kinetics based on environmental conditions allows for maximising dehydrated tomato production, enhancing food security.

KEYWORDS

Environmental conditions, Dehydrated tomato, Solar dryer, Forced convection, Drying kinetics, Temperature control, Tomato drying kinetics.

INTRODUCTION

Due to its high nutritional value, such as content of antioxidants, vitamins A, C, and E, proteins, etc., the tomato (*Lycopersicon esculentum*) [1] is one of the most cultivated and consumed foods in the world [2]. In 2023, global tomato production increased by 25% compared to 2010. The total product was 192 million tons per year [3], and 32% was wasted [4]. Tomato is among the ten most consumed foods in the Mexican diet. In the last 10 years, production grew an average of 9.5%, reaching an amount of up to 3 million tons per year in 2023 [5]. However, tomato losses per year in Mexico have remained around 39.3% [6], so tomato in Mexico represents one of the crops with the highest economic losses due to waste. 15.2% of producers attribute these losses to a lack of knowledge about preservation methods. This situation highlights the need for training in postharvest preservation techniques [6]. In environmental terms, this waste means that for every 0.453 kg of wasted tomatoes, 1.13 kg of CO₂eq are produced [4].

* Corresponding author

The gap between the amount of food produced and consumed by the population highlights the need for solutions such as food dehydration. This process minimises food waste by extending the product's shelf life and maximises producer profits by opening up new business opportunities. It is also an alternative that guarantees food security in terms of availability, access, and stability, especially in rural and marginalised communities with limited resources. According to Shamah-Levy *et al.* [7], in 2023, approximately 44.6% of Mexican households reported some degree of food insecurity.

Dehydration is a viable alternative for preserving perishable tomatoes. Dehydrated products retain their nutritional value and improve their storability [8] by significantly reducing their volume [9]. In addition, their economic value can increase by up to 98% compared to the cost of the original raw material [10]. Dehydration plays a key role in food safety, as it extends the shelf life of products and ensures their availability. It represents an opportunity to meet the dietary needs and preferences of consumers, promoting healthy and affordable eating for a healthy life [11].

In traditional drying, solar radiation interacts directly with the product lying on a surface exposed to the environment. However, this technique has disadvantages such as long drying times, use of large surfaces, exposure to weather conditions, lack of control of operating conditions, risk of contamination and alterations in the colour of dehydrated agricultural products [12], as well as theft [13]. This situation is the reason why conventional dehydration has emerged. Here, the food is protected in a drying chamber, and the air is heated by burning fossil fuels or by using electrical resistors powered by this same source [14]. It guarantees a constant and continuous supply of energy, allowing control of the process conditions. However, this practice contravenes Sustainable Development Goal 13 (SDG 13) for the decarbonisation of the planet [15], since up to 40.2 kg of CO₂ are produced per kilogram of dehydrated tomato [16].

Solar energy is a renewable, clean, cost-free, and accessible energy source for the entire population. Mexico's geographic location is 23°38'4.2" N, 102°33.167' W, with an average solar radiation of 5.5 kWh/m² and radiation exceeding 8 kWh/m² in spring and summer in the northwest of the country. A high solar potential favours solar drying of fruits and vegetables year-round.

Indirect solar drying with forced convection has proven effective in reducing spoilage and improving product quality [17]. Indirect solar dryers consist of a drying chamber and a solar air collector, which preheats the air before introducing it into the drying area [12], preserving food safety and improving the quality of the final product [18]. This technique also promotes a more controlled and efficient process and protects the product from weather and theft.

Several investigations on indirect solar dehydrators with forced convection have been published in the open literature. Suherman *et al.* [19] carried out the dehydration of tomato slices. They found that the drying was faster compared to sun drying. The drying rate is influenced by air speed and temperature, product type and moisture content. The moisture content decreased from 94% to 25% and 58%. Sharma *et al.* [20] dehydrated 3 kg of tomato slices in 10 hours, with irradiance levels ranging from 424 to 670 W/m². They did not report the drying temperature, but published that the drying efficiency was 41%. Cetina *et al.* [21] dehydrated 4 kg of tomato slices during December 2018 and January 2019, with maximum irradiance levels of 837 W/m². The maximum drying temperature was 35.7 °C. The drying time was 25 hours. Chouikhi and Amer [22] evaluated the performance of a dehydrator by drying 250 g of tomato slices. The moisture content was reduced from 92% to 10% over two days (8 hours per day), at irradiance ranges of 600 to 670 W/m². The air temperature inside the dehydrator was variable, recording between 29.8 and 42 °C. Tera *et al.* [23] performed the drying of 2.2 kg of tomato slices. The experimental results showed that the moisture content on a dry basis was reduced from 17.6 kg/kg dry solid to 0.12 kg/kg dry solid in 40 h. Abuelnuor *et al.* [24] found that the drying time of 221 g of tomato was 10 h.

The reviewed studies show that the drying times for tomato slices dehydration vary widely, ranging from 8 h to 40 h for loads of 221 g to 4 kg. The cited researchers did not conduct a quantitative evaluation of the impact of meteorological variables on drying kinetics and process efficiency, which directly influences drying duration.

Despite their operational advantages, the performance of indirect solar drying systems is influenced by various factors, such as air speed, solar radiation, and ambient relative humidity, most of which cannot be controlled [25]. This lack of control represents one of the main challenges in the development of solar systems. The study of environmental conditions is essential to determine the relationships between them, the ranges in which their values vary, the impact they have on the drying kinetics and the operating conditions of the solar dehydrator. Noori *et al.* [26] dehydrated 3 kg of tomato slices in an indirect solar dehydrator with forced convection. They found that the moisture content decreased from 92% to 22% in a drying time of 30 h under winter conditions, while during the summer, the drying time was reduced from 15 to 25 h. Without quantifying the relationship between the environmental variables, they observed that the drying rate is affected by the variation in irradiance, temperature and relative humidity. Silva [27] evaluated the performance of an indirect solar dehydrator using plantain in two cities in Brazil. Four experimental tests were carried out under different climatic conditions, during the summer and winter seasons. Although the study does not present a detailed quantitative analysis of environmental variables, the results indicate that high temperatures and low relative humidity in summer favoured the drying process, reducing drying time by up to 31% compared to winter conditions. Benseddik *et al.* [28] performed an analysis of meteorological variables (irradiance, ambient temperature, and relative humidity) in 7 Algerian cities using isopleth plots. The study did not demonstrate experimentally or numerically which of the 7 cities had the shortest drying time. The only conclusion was that the drying process is favoured in desert cities with irradiance, ambient temperature, and relative humidity values of 1200 W/m², 45 °C, and 10%, respectively. Olmos-Cruz *et al.* [29] performed an analysis of 876,000 data points corresponding to the four main environmental variables (ambient temperature, relative humidity, wind speed and irradiance) during the year 2023, introducing a graphical tool based on statistical values such as box diagrams (boxplot). The authors quantitatively determined the impact of these environmental variables during the annual apple drying. It was found that irradiance, followed by relative humidity and ambient temperature, affects the drying kinetics, with April being the month with the shortest drying time of 5.0 h. In contrast, in winter, drying times increased by up to 40%.

The analysis of environmental variables during tomato dehydration allows for controlling drying temperature, regulating dehydrator energy use, and minimising heat losses from the equipment. This approach improves drying kinetics and significantly reduces drying time, which impacts profitability, production, and the quality of the dehydrated product. The present work uses a box plot as a graphical tool for the thermodynamic study of environmental variables that maximise tomato drying kinetics and process efficiency, while minimising drying time. Six experimental tests, covering the four seasons of 2024, were conducted with 10 kg of tomato in an indirect solar and forced convection dehydrator at a controlled operating temperature of 50 °C and an air mass flow rate of 0.7 kg/s. Characterising drying kinetics based on environmental conditions allows for maximising dehydrated tomato production and improving food safety.

CHARACTERISATION OF TOMATO DRYING KINETICS, BASED ON VARIABILITY OF ENVIRONMENTAL CONDITIONS

The relationship between environmental variables during tomato dehydration directly affects drying kinetics. The study of these variables contributes to understanding the solar device in all four seasons, achieving competitive drying efficiencies and drying times that promote production capacity. This section addresses conceptual aspects and procedures to

determine the relationship between the four selected environmental variables that intervene during the drying process.

Description of the solar device

An indirect solar dehydrator was used. The drying air is heated indirectly by solar collectors. This system allows temperatures above 85 °C to be reached in the winter season (Northern Hemisphere) and maintains temperature control during the day. Once the air reaches the desired temperature, it flows into the drying chamber. The dehydrator has a capacity of 10 kg of tomato fruits per batch. The air removes moisture by forced convection at a speed of 5.0 m/s. **Table 1** shows the instrumentation used to monitor drying conditions. The device is located on the solar platform of the Pueblito de Rocha Campus, at the University of Guanajuato, city of Guanajuato, Mexico, coordinates 21°01'36"N, 101°16'10"W.

Table 1. Solar device instrumentation

Parameter	Symbol	Unit	Instrument	Model	Resolution	Range
Temperature	T	°C	Sensor	DHT-22	0.1	−40 to 125
Relative humidity	HR	%	Sensor	DHT-22	0.1	0 to 100
Air speed	V	m/s	Anemometer	Kethvoz KE-846	0.01	0.3 to 45

Tomato preparation

The tomato used is of the lowest quality on the national market. Washing and sanitising are carried out in a sanitising room, using the botanical disinfectant RBM-TC®, at a concentration of 200 ppm. The residence time of the tomato in the disinfectant solution is 40 seconds. The tomato fruits are cut into wedges. The average measurements of the fresh tomato cuts are: mass of around 0.0218 kg ± 0.000002 kg, and dimensions 3.4 cm wide, 5.6 cm long and 2.4 cm high, with an uncertainty of ± 0.02 cm. The surface of the cut tomato is covered with sodium chloride, which acts as an absorbent agent, facilitating the removal of water and preventing the proliferation of fungi. The dehydrator is loaded with 10 kg of tomato prepared in this way.

Experimental tests

Six experimental tests were conducted during four seasons of the year 2024: January 14th, February 7th, March 13th, June 12th, August 19th, and November 1st. The methodology, schematically shown in **Figure 1** and described below, was followed for each drying test.

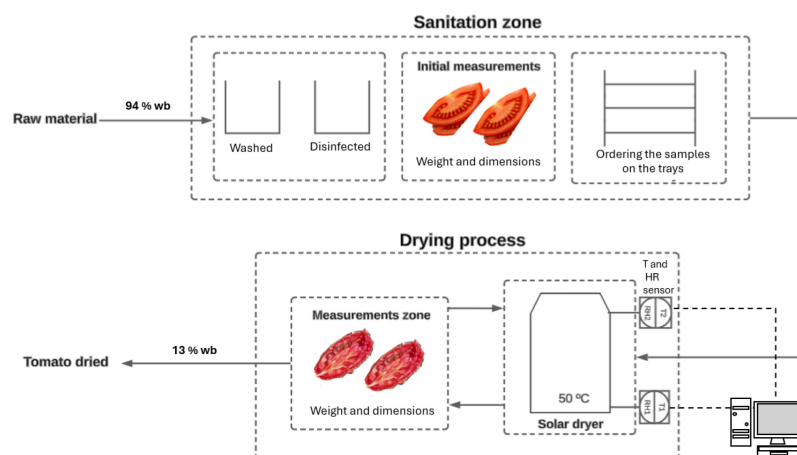


Figure 1. Process diagram: tomato preparation and drying

Before each test, the solar dehydrator is preheated, and simultaneously, the 10 kg of tomatoes to be dehydrated are prepared as indicated in the "Tomato preparation" section. The tomatoes are loaded into the dehydrator once the heated air reaches the target temperature of 50 °C, around 9:30 h. The air speed is 5.0 ± 0.017 m/s (which is equivalent to an average flow rate of 0.7 kg/s) for each test. This speed remains constant throughout the test. The test concludes when the moisture content of the samples is 2.54 g/g dry matter. The target temperature and relative humidity in the dehydrator are recorded every minute during the drying process. **Figure 1** represents the procedure followed for the preparation of tomatoes and experimentation. **Table 1** describes the specifications of the measuring instruments used to measure the mass and dimensions of the tomato samples.

Table 2. Measuring instruments

Parameter	Symbol	Unit	Instrument	Model	Resolution	Range
Sample mass	m	g	Analytical balance	CGOLDEN WALL 500	0.001	0 to 500
Sample radius	r	mm	Digital Vernier	KEATRONIC	0.01	0 to 150
Sample thickness	z	mm	Digital Vernier	KEATRONIC	0.01	0 to 150

Graphical method: boxplot

An analysis of environmental conditions is used to evaluate the behaviour of the solar dehydrator during the day, the season, and the year. The final combined effect of environmental conditions is reflected in the operating conditions of the solar dehydrator and, therefore, in the drying kinetics. To evaluate in detail, a graphical method of descriptive statistics called a boxplot (otherwise known as a box and whisker plot or diagram) was applied. The analysis determined the relationship between environmental factors and their influence on the drying rate of the tomato's moisture content. This analysis guarantees the supply of the heat load and control of the operating conditions in the solar dehydrator during dehydration time.

Boxplot diagrams use the median, mean, and interquartile range (IQR) to evaluate symmetry, dispersion, bias, and the presence of outliers in a set of data ordered from lowest to highest [30]. The most critical environmental conditions in solar dehydration are ambient temperature, relative humidity, wind speed, and irradiance. The construction of boxplot diagrams (**Figure 2**) for each of these variables allows us to evaluate the central tendency of the data, its variability and distribution patterns, as well as outliers by calculating the IQR dispersion.

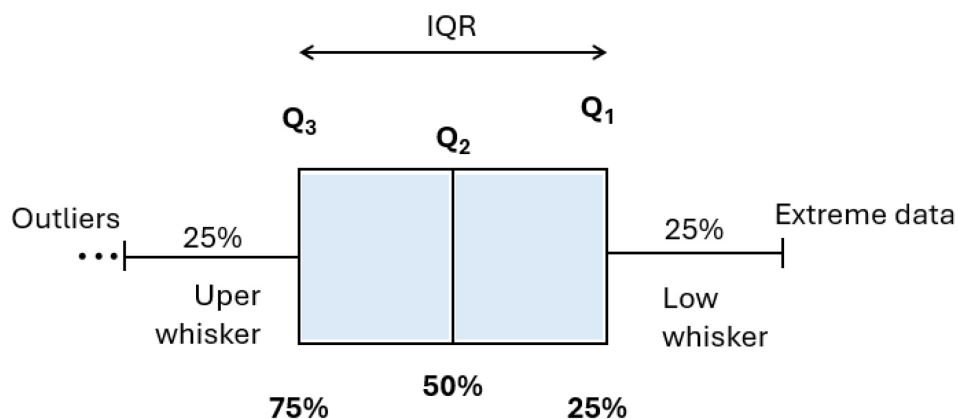


Figure 2. Boxplot diagram

The IQR is the result of the difference between the third quartile (Q_3) and the first quartile (Q_1). Quartiles are determined with eq. (1):

$$Q_k = \frac{a(N+1)}{100} \quad (1)$$

where N is the number of data points and a is the percentile value to calculate (25, 50, and 75).

Both the Q_1 and Q_3 quartiles separate the lower and upper 25% of the data, respectively. These quartiles are known as the 25th and 75th percentiles, and together they form the box. The Q_2 quartile (50th percentile) corresponds to the centre line of the box and indicates the median. The whiskers (lines outside the box) show the extension of the range of the remaining 50% of the data, that is, they start from the Q_1 and Q_3 quartiles to the minimum and maximum values of the data. The whisker is 1.5 times the IQR [30]. Outliers are individual points that lie outside the whiskers and represent values that deviate significantly from the rest of the data set due to measurement errors or unusual events (atypical data).

A total of 28,800 data points were analysed for the four main environmental variables in dehydration (ambient temperature, relative humidity, wind speed, and irradiance), obtained between 8 and 18 h, during six drying tests in 2024 in the city of Guanajuato, Mexico. It is equivalent to a total of 600 data points per variable per day. The range, in which the environmental conditions were measured, is considered adequate, since irradiance decreases by up to 87% after 17:35 h [29].

Drying kinetics

In tomato dehydration, complex heat and mass transfer phenomena co-occur during the process. The wet solid removes thermal energy by convection of the hot air, part of which is used on the surface of the product to evaporate free water. At the same time, the rest is transferred by conduction to the interior of the wet solid, which increases the temperature and promotes mass transfer by diffusion.

The moisture content of the solid (or absolute humidity) is expressed on a dry basis (db) or a wet basis (wb). In the calculations of the dehydration of a food, it is convenient to refer to the moisture content on a dry basis, M_{db} , [g of water per g dry matter] since this remains constant throughout the process [31] and is calculated with eq. (2):

$$M_{db} = \frac{m_o - m_d}{m_d} \quad (2)$$

where m_o and m_d are the initial mass of fresh food and the mass of the dry product [g], which are obtained by weighing the samples with an analytical balance [32].

To calculate the dry mass of the dehydrated tomato, the samples were dried in a Yamato DX 302 drying oven at a temperature of 105 °C for 24 hours. Subsequently, they were allowed to cool in desiccators and were weighed. Variation of absolute humidity of the product, $DM_{(db)}$, as the dehydration process progresses, it is given by eq. (3):

$$DM_{(db)} = \frac{m_t - m_d}{m_o} \quad (3)$$

where m_t is the sample mass, [g], as the drying process is occurring.

The drying rate DR , at which the moisture content of the product is removed, is expressed with eq. (4):

$$DR = \frac{dM_{db}}{dt} = \frac{M_t - M_{t+\Delta t}}{\Delta t} \quad (4)$$

where $M_{t+\Delta t}$ is the moisture content (on a dry basis) after an increase in time Δt [h].

The effective diffusion coefficient (D_{eff}) is a parameter that describes the drying kinetics, since it determines the speed of the process during the decreasing drying rate. In this decreasing period, the free water on the surface of the material has already completely evaporated, and a concentration gradient is formed between the inner and outer parts of the food. The moisture content diffuses from the centre to the surface and is described by Fick's Second Law [33]. The variables affecting the kinetics are related to temperature, relative humidity and drying air speed, as well as the geometry and moisture content of the sample [34]. The tomato was cut into wedges; that is, radial cuts were made from the centre to the edge. Each wedge is considered to consist of two flat plates, and the dehydrated tomato is the sum of the two flat plates. The circular edges of the dehydrated fruit shrink and curl, forming a straight line. The same occurs with the circular ends. That is, considering that the solid flat tomato slices experience continuous drying, there is a uniform distribution of moisture and a considerable concentration on the surface of the sample at the beginning of the process.

Considering the constant and non-shrinking material characteristics, and the fact that evaporation occurs only on the surface of the sample and the mass transfer is symmetrical and uniform throughout the drying process [35], the effective diffusion coefficient can be calculated through eq. (5):

$$\frac{\partial M_{db}}{\partial t} = D_{eff} \left(\frac{\partial^2 M_{db}}{\partial x^2} \right) \quad (5)$$

where M_{db} is the moisture content of the tomato on a wet basis, D_{eff} is the effective diffusion coefficient, x is the position within the plate, and t is time. M_{db} (moisture content on a dry basis) will be represented in the following equations simply as M to simplify the nomenclature.

Considering that there is no diffusion through the peel of the tomato, Xu *et al.* [36] concluded that the peel is a dynamic barrier against desiccation (water loss) and microbial invasion. Ji *et al.* [37] reported that impermeable peel defines the effectiveness of postharvest processing.

Eq. (5) is subject to the boundary and initial conditions specified below, where R is the initial thickness of fresh food and M_e is the equilibrium moisture content:

- when $t = 0$ and $0 < x < R$; eq. (6):

$$M = M_o \quad (6)$$

- when $x = 0$ and $t > 0$; eq. (7):

$$\frac{\partial M}{\partial r} = 0 \quad (7)$$

- when $x = R$ and $t > 0$; eq. (8):

$$M = M_e \quad (8)$$

The analytical solution of the governing equation (5), proposed by Crank [38] but simplified by considering long drying times [39], is represented here by eq. (9):

$$M_r = \frac{8}{\pi^2} \sum_{i=0}^{\infty} \frac{1}{(2i+1)^2} \exp \left[-(2i+1)^2 \pi^2 \frac{D_{eff}}{L^2} t \right] \quad (9)$$

where L is the thickness of the flat wedge and M_r is the moisture removal rate (on a dry basis). Eq. (10) relates the current moisture gradient at time t (M_t), with the maximum gradient that exists in the drying system:

$$M_r = \frac{M_t - M_e}{M_o - M_e} = \frac{M_t}{M_o} \quad (10)$$

where M_o and M_e denote the initial and equilibrium moisture content on a dry basis. The latter represents a very small value compared to M_o and M_t .

Drying efficiency

The drying efficiency (η_d) of the dehydrator is calculated with eq. (11), where E_{evap} is the energy required to evaporate the free moisture from the food, eq. (12), and E_{in} is the total solar energy used in the dehydrator, eq. (13):

$$\eta_d = \frac{E_{evap}}{E_{in}} \quad (11)$$

$$E_{evap} = m_w \lambda_{vap} \quad (12)$$

$$E_{in} = G \times A \times t_d \quad (13)$$

where m_w is the total mass of water evaporated [kg], λ_{vap} is the latent heat of vaporisation of free water [kJ/kg], G is irradiance [kW/m²], A is absorber area [m²], and t_d is the total drying time [s].

Carbon dioxide removal

The amount of CO₂ emissions released during drying by a conventional tomato dehydrator is calculated using equation (14):

$$em_{CO_2} = \dot{M}_{ng} \times t_d \times F_{em} \quad (14)$$

where \dot{M}_{ng} is the natural gas mass flow rate [kg/s], and F_{em} is the average emission factor for natural gas, equal to 2.69 kg CO₂/kg natural gas [40].

Calculation of uncertainty

In solar dehydration experiments, it is essential to estimate the uncertainty of independent variables such as target temperature, air speed, mass and geometric dimensions of the sample, in addition to derived parameters such as heat and mass transfer coefficient and shrinkage, among others.

The uncertainty (F) is determined from eq. (15), which is a function of the uncertainty of the independent variables ($x_1, x_2, x_3, \dots, x_n$) [41]:

$$F = \left[\left(\frac{\partial F}{\partial x_1} w_1 \right)^2 + \left(\frac{\partial F}{\partial x_2} w_2 \right)^2 + \left(\frac{\partial F}{\partial x_3} w_3 \right)^2 + \dots + \left(\frac{\partial F}{\partial x_n} w_n \right)^2 \right]^{1/2} \quad (15)$$

where w_1 to w_n are the estimated uncertainties of each measured variable, resulting from the minimum resolution of each instrument, reported in Table 1 and Table 2.

Devices with an uncertainty of less than or equal to 5% are considered adequate according to the standards [22].

RESULTS

This section presents the results obtained from the statistical analysis of the boxplot applied to the study of the environmental conditions existing during each of the tests carried out during the 4 seasons of the year 2024. In addition, the joint impact of the environmental variables on the kinetics and efficiency of drying is described.

Graphical analysis: boxplot method

Figure 3 shows the ambient temperature trend during the tests. June 12th was the test with the highest temperature values. The average maximum value was 31.38 °C and the minimum value was 20.44 °C. The interquartile range was 4.05 °C, where temperatures within the box (50% of the data) ranged from 25.5 °C to 29.3 °C. June 12th exhibited a positive skew, that is, mean > median > mode. This situation means that the middle 25% of the data clustered in the upper part of the box (from Q_2 to Q_3) with temperatures between 28 and 29.3 °C, while the data below the median showed a greater dispersion, tending toward temperature values between 25.5 and 28 °C. The November 1st test is negatively skewed (mean < median < mode) because the data cluster at the bottom of the box (Q_1 to Q_2), creating a concentration of data below the median between 11.35 and 14.7 °C. The IQR within the bottom 50% of the data in the box is 12.16 °C, with the Q_3 quartile temperature at 23.5 °C. November 1st had the lowest temperatures in the bottom 50% of the data, with values of 11.35 °C (Q_1).

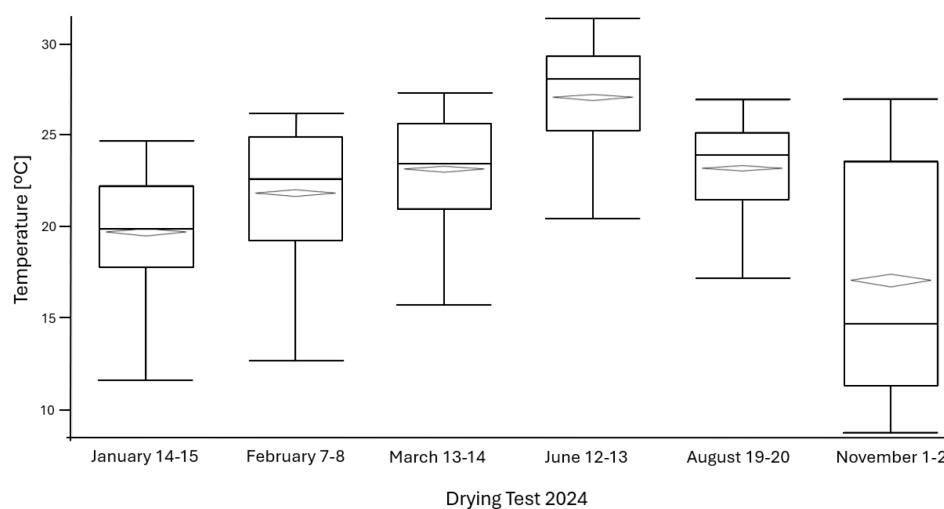


Figure 3. Boxplot diagrams of ambient temperatures

The median for each month shows notable differences, with minimum and maximum temperature values of 14.7 °C and 28.02 °C corresponding to November 1st and June 12th, respectively. The mean represents the average of the data contained within the box and is represented by the diamond (Figure 3). This trend varies, as does the median, to the point of overlapping. That is, for January 14th, the mean and median differed by 0.92 °C, demonstrating

a symmetry in the data on this day. November 1st showed the greatest asymmetry, with a difference between its mean and median of 2.4 °C.

Figure 4 shows the box-and-whisker plot describing the behaviour of relative humidity. During the first four tests, low relative humidity levels were present, ranging from 15.3 to 32%, with median values of 27.9, 21.6, 27.3, and 30% for the tests on January 14th, February 7th, March 13th, and June 12th, respectively. The February 7th was shown to be the test day with the lowest relative humidity levels, with 50% of its data hovering between 16.67% and 27.17% (Q_1 and Q_3). It exhibits a positive bias, with a difference between the mean and median of 1.82 °C. The number of atypical data points during February was 53, all of which are above a relative humidity of 42.9%.

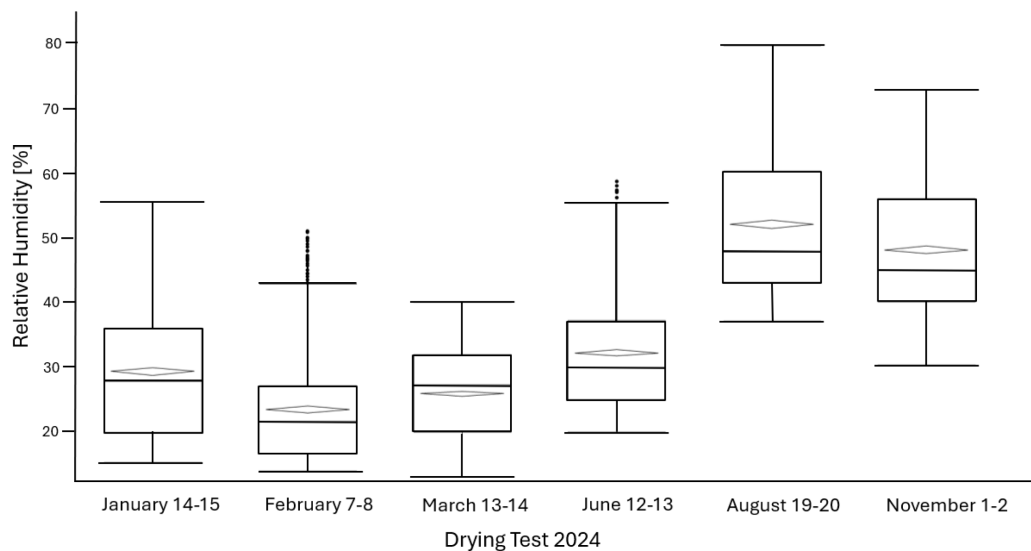


Figure 4. Boxplot diagrams of relative humidity

The median for January 14th, March 13th, and June 12th showed a similar trend, ranging from 27.3 to 30%. June showed the greatest asymmetry with a difference between its mean and median of 2.2% and 11 outliers, which are above the extreme figure of 55.67%. On the other hand, the tests for August 19th and November 1st showed an increase of up to 61.5 % compared to February 7th, with relative humidities between 40.1 % and 60.25%. August 19th was the day with the highest percentage values of relative humidity, where 50% of its data are between 43.28% and 60.25% (Q_1 and Q_3), followed by November 1st with values ranging between 40.08% and 56%. The data from August 19th showed a positive skew with a difference between its mean and median of 4.7% and 3.1% on November 1st.

Figure 5 shows the boxplot diagram for wind speed. It can be seen that 50% of the data in each box is symmetrical, as the difference between the mean and median averages is 0.77 m/s. The average for the months shown ranges between 2.48 and 3.18 m/s.

Like relative humidity, the tests on January 14th, February 7th, and March 13th show the highest wind speeds. The middle 50% of the data for these tests ranged between 1.78 and 4.19 m/s. The test conducted on March 13th showed the greatest data dispersion (IQR) with a value of 1.99 m/s, with a maximum wind speed of up to 7.7 m/s. Fifty percent of their data fall within the range of 2.2 m/s to 4.19 m/s (Q_1 and Q_3).

June 12th, August 19th, and November 1st recorded the lowest wind speeds, with a reduction of up to 47%. The middle 50% of the data show speeds ranging from 1.3 to 3.2 m/s. A greater concentration of data is observed for these months, with IQR ranges of 0.94, 1.1, and 1.34 m/s for August, November, and June, respectively. Like the three previous tests, the median for August 19th and November 1st tends toward a speed value of 2 m/s. The August 19th test recorded the lowest levels on record, with 50% of its data falling within the range of 1.35 m/s to

2.28 m/s (Q_1 and Q_3 , respectively), representing a variation of 0.935 °C and a 2.12-fold shorter case length compared to March 13th.

The largest number of outliers occurred on June 12th with 41, followed by November 1st with 25, and August 19th with 24.

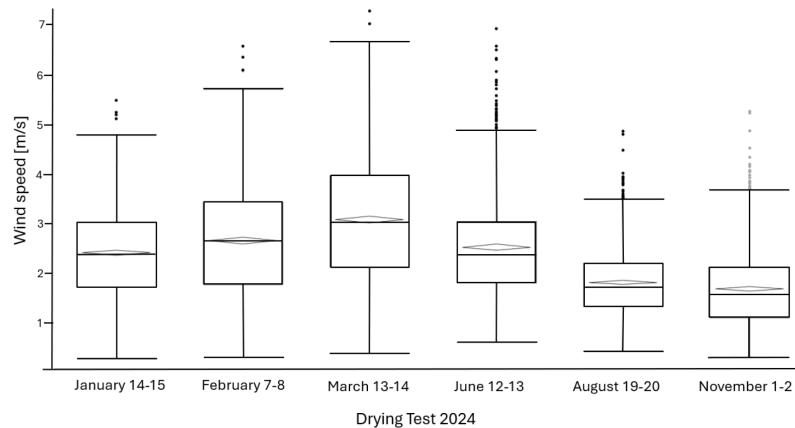


Figure 5. Boxplot diagrams of wind speed

Figure 6 shows the diagram for the irradiance of the tests carried out during the year 2024. The behaviour of this variable is parabolic throughout the year. The dispersion of the data in the boxes of each test is considerably high, with values of IQR up to 566 W/m², as is the case with the test of August 19th. The boxes present symmetry, the difference between the average mean and median is 16.9 W/m², with the difference in August being the smallest of all the tests, with a value of 0.6 W/m². June presented the greatest dispersion with 20.2 W/m².

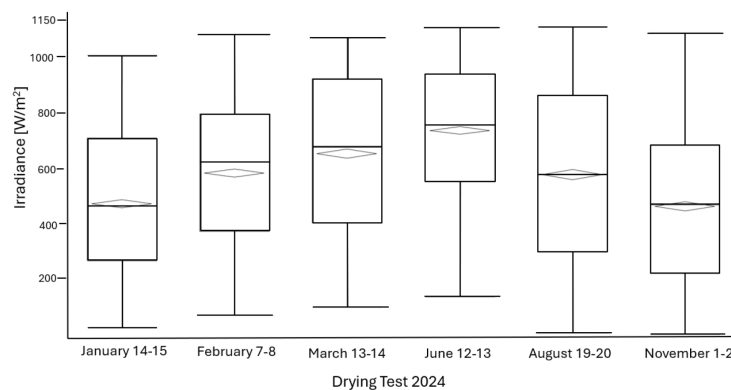


Figure 6. Boxplot diagrams of irradiance

The tests carried out in November presented the lowest levels of irradiance. 50% of the data was concentrated between 220.2 and 680 W/m² (Q_1 and Q_3 , respectively), which represents a variation of 459.7 W/m². The box presents symmetry with a difference between the mean and median of 4.6 W/m². During the test, there was high cloudiness, reducing the irradiance level by up to 99% for a time of 1.7 h.

The highest irradiance levels were in June. 50% of the data is concentrated in values from 549 to 938 W/m². The box presents the lowest data dispersion with an IQR of 389 W/m² compared to August, which had the highest data dispersion with an IQR value of 566 W/m², and with a box length of 1.45 times larger than that of June.

The data dispersion with the highest average irradiance levels and average ambient temperature was on June 12th, with 769 W/m² and 27.2 °C, respectively. Relative humidity showed an increase of 31.4% compared to the humidity of March 13th, which has an average value of 24.5% and wind speeds of up to 3.28 m/s, being 1.15 times higher than the values

recorded for June 12th. The dehydration on March 13th presented the shortest drying time of 9.6 h (Day 1: 5.07 h, and Day 2: 4.57 h), with a lower level of irradiance and ambient temperature (680 W/m² and 24.8 °C).

The February 7th run was the next test with the shortest drying time of 11.7 h (day 1: 6.5 h, and day 2: 5.1 h). The average relative humidity and wind speed levels were below those recorded on March 13th, with values of 9.3% and 14.2%, respectively. The average irradiance level recorded in the test was 580.5 W/m², being 1.12 times lower than that recorded in the March 13th test.

Uncertainty analysis

The results of the uncertainty calculation are presented in [Table 3](#) for the measuring instruments such as the analytical balance, digital vernier and sensors. In each evaluation, the factors due to i) the instrument, ii) the readings, iii) the air leaks, iv) the connection, and v) the loss of material in the trays were considered.

The total uncertainty in the experimental measurement ($W_{ex,total}$) is $\pm 0.26\%$, which is below the 5% considered as the acceptable limit for measuring devices [\[22\]](#).

Table 3. Uncertainty values

Parameter	Calculated uncertainty
Drying temperature	$W_{T,total} = \pm 0.2$
Relative humidity	$W_{HR,total} = \pm 0.17$
Air speed	$W_{V,total} = \pm 0.017$
Sample mass	$W_{w,total} = \pm 0.002$
Dimensions	$W_{D,total} = \pm 0.02$

Drying kinetics

Solar dehydration of 10 kg of tomato was carried out at a controlled temperature of 50 °C for each of the tests during the four seasons of 2024 using an indirect, tower-type, forced-convection solar dehydrator. The six experimental runs, whose dates were randomly selected, were carried out on January 14th, February 7th, March 13th, June 12th, August 19th, and November 1st. The average drying time was 9 hours.

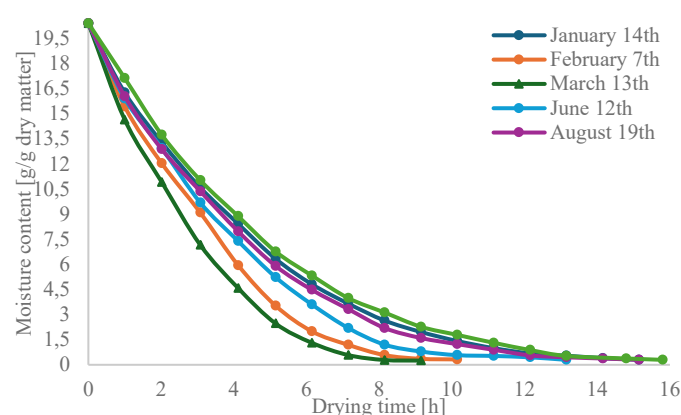


Figure 7. Loss of moisture content in tomatoes

Figure 7 shows the curve of the average moisture loss of the tomato samples (dry basis) with respect to the drying time. This test was carried out on March 13th and 14th, with a drying time of 9.6 hours. The drying rate on the same day varied significantly compared to March 14th, with the samples losing 70% of their free water on March 13th (5.0 h), dropping from 19.79 to

5.18 g water/g dry matter. On the second day (4.57 h), the moisture loss of 38.6% occurred, reducing their moisture content from 5.18 to 2.50 g water/g dry matter. The overall free water loss was 81.7%.

Figure 7 also shows the average moisture loss curve for the November 1st test, which had a drying time of 15.9 h. On day 1, the drying time was 8.3 h, and the samples lost about 63% of their free water, going from 20.6 to 6.09 g water/g dry matter. On the second day, the drying time was 7.6 h, and the moisture loss was 49.5%, reducing their dry matter moisture content from 6.09 to 2.55 g water/g dry matter. In addition, the evaporation rate was 0.924 kg/h, 1.85 times lower than the tests performed on March 13th.

The environmental conditions for March 13th and 14th are shown in **Figure 8**. **Figure 8** shows that March 13th experienced fluctuations in irradiance levels starting at 14:15 h and continuing for 2.3 hours, recording a minimum irradiance value of up to 160.3 W/m². The minimum ambient temperature and maximum relative humidity recorded during this intermittent period were 24.35 °C and 26.7%.

March 14th (**Figure 8b**) experienced smaller irradiance fluctuations compared to the previous day. The average values for March 14th were: 698.67 W/m² irradiance, 23.5 °C ambient temperature, and 24.32% relative humidity. The moisture content of the tomato was reduced from 20.58 to 2.5 g/g dry matter, representing a drying rate of 1.7 kg/h evaporated water and a moisture removal rate from 1 to 0.014.

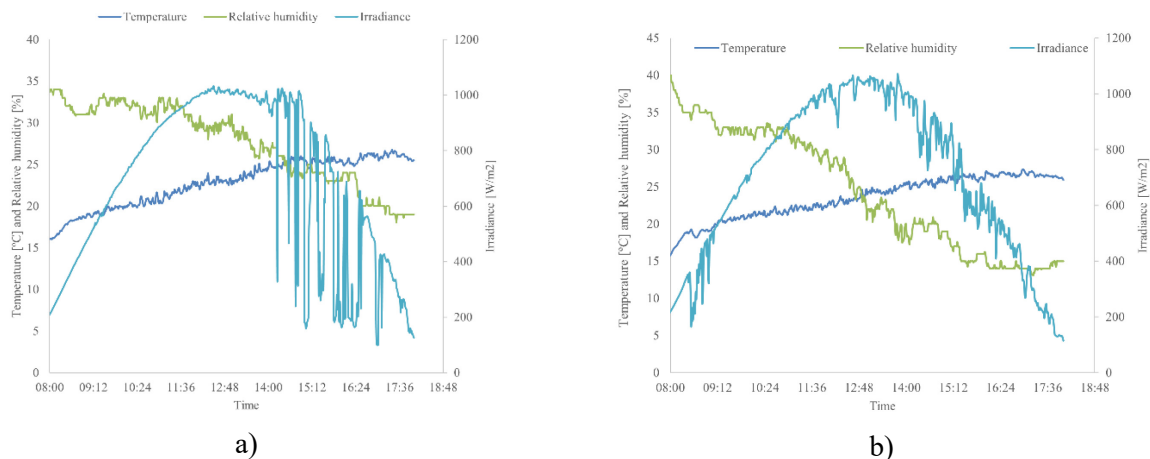


Figure 8. Irradiance curve and ambient temperature and relative humidity for March 13th (a), and March 14th (b)

The test with the longest drying time was conducted on November 1st and 2nd. The total drying time was 15.8 h (day 1: 8.3 h, and day 2: 7.5 h). The environmental conditions for this test are shown in **Figure 9**. **Figure 9a** shows irradiance fluctuations, as in March. However, the first day showed significant fluctuations in solar irradiance, beginning at 11:11 h and ending at 14:57 h. Irradiance decreased by up to 66% during this period of solar intermittence. On the other hand, ambient temperature and relative humidity remained constant during the period of minimum irradiance, at 23.8 °C and 40%.

On the second day (**Figure 9b**), irradiance fluctuations were again observed, with an average value during the day of 500.4 W/m². The average ambient temperature and relative humidity were 22.1 °C and 50.9%, respectively. However, the relative humidity was 11.1% higher than the previous day. The second day required 7.6 h to evaporate 49.5% of the moisture content, which is 1.27 times less than the amount of water evaporated on the first day, thus reaching the final moisture content of 2.55 g water/g dry matter.

The drying time for the tests was 11.7 h for February 7th, 13.0 h for June 12th, 15.0 h for August 19th, and 15.4 h for January 14th.

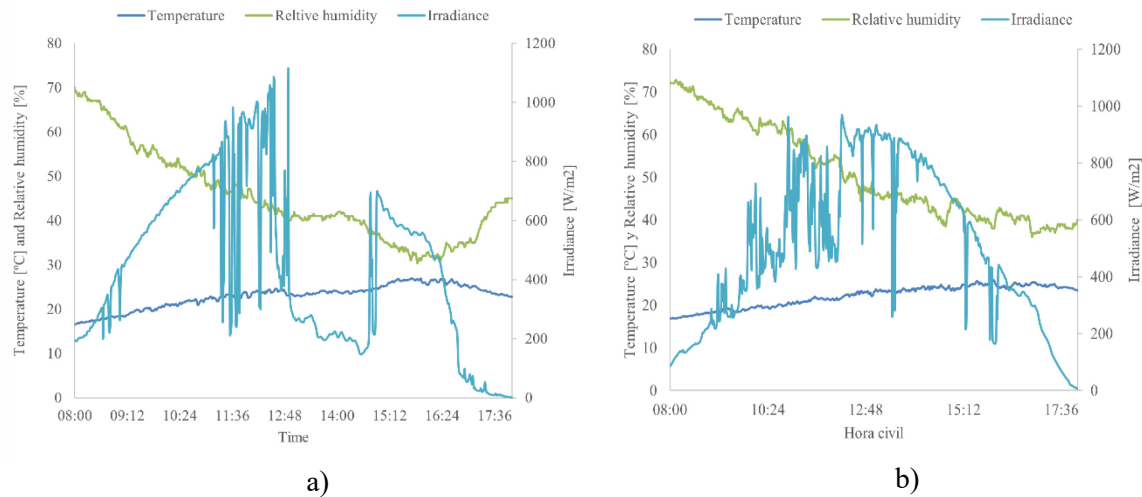


Figure 9. Irradiance curve and ambient temperature & relative humidity for November 1st (a) and November 2nd (b)

Figure 10 shows the drying rate (on a dry basis) versus time for each test. The amount of moisture evaporated from the tomato over a given period was graphed. Only the decreasing drying period is presented because neither the heating phase nor the constant drying period was observed. This behaviour was also found by Abuelnuor *et al.* [24], Fterich *et al.* [35], Nettari *et al.* [41], and Mühlbauer and Müller [42]. The critical moisture content (M_c) corresponds to the initial point of each test, which is between 4.8 and 3.81 g/g dry matter-h, with March 13th and November 1st being the tests with the shortest and longest drying times, respectively. In the first hours of drying, the evaporation of the free moisture content decreases rapidly. The high drying rates decrease towards the final hours of the process due to the lower residual moisture content in the products, reaching a value of 1.10 g/g dry matter-h.

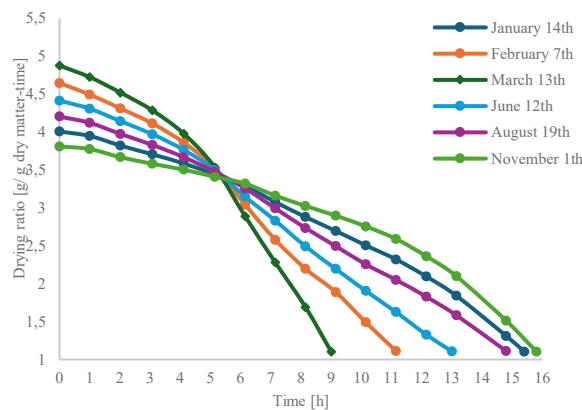


Figure 10. Drying rate vs time

The average effective diffusion coefficient D_{eff} for tomatoes for the March 13th trial was $8.01 \times 10^{-10} \text{ m}^2/\text{s}$. For the longer drying trials, on November 1st and January 14th, D_{eff} values were 1.76×10^{-10} and $3.62 \times 10^{-10} \text{ m}^2/\text{s}$, respectively. These values are higher than those reported by Fterich *et al.* [35], Badaoui *et al.* [39], and Nettari *et al.* [41], who used forced convection solar devices with variable operating temperatures ranging from 40 to 70 °C and with speeds of 1 m/s to 3 m/s.

CO2 analysis

The implementation of this indirect solar dehydrator allows for a significant reduction in CO₂ emissions, thus contributing to more sustainable production. For a 10 kg batch of fresh tomatoes, 0.15 kg/h of natural gas is consumed in a conventional gas dryer. For a 12-hour

average drying operation per batch for 360 days per year, 648 kg of natural gas is consumed per year, equivalent to a total of 1.75 tons of CO₂ per year. If the solar dehydrator had a useful life of 20 years, then 35 tons of CO₂ would be eliminated. Sharma *et al.* [20] determined that their solar dehydrator can eliminate up to 12.28 tons of CO₂ emissions.

Temperature control

Temperature control was carried out during the six tomato trials conducted in 2024. For the tomato trial conducted on March 13th, Figure 11 shows the temperature of the drying air entering and leaving the indirect solar dehydrator. The experimentation without tomatoes was carried out at the beginning of each test during the preheating phase for 1 hour. The temperature was measured at the inlet and outlet of the drying chamber. The average temperature difference between both measurements was 4.22°C, which corresponds to an average heat loss of 2.97 kW.

The target temperature of 50 °C was reached at 9:10 h (blue line). The drying temperature was maintained for up to 6.5 h throughout the entire test. The batch of 10 kg enters at 9:30 h. The air temperature recorded at the dehydrator outlet (green colour) is 1.3 times lower than the target temperature, due to the removal of moisture content from the tomato. As the drying process progresses, the air temperature at the dehydrator outlet increases due to the decreased removal of moisture content.

During each sampling, the exhaust fan is turned off and the drying chamber door is opened. This causes the drying chamber temperature to drop suddenly, as shown in Figure 11. Once the sampling is complete, the sample trays are loaded in, and the process temperature is restored to 50 °C in an average time of 6 min. This behaviour was repeated in the other experimental tests.

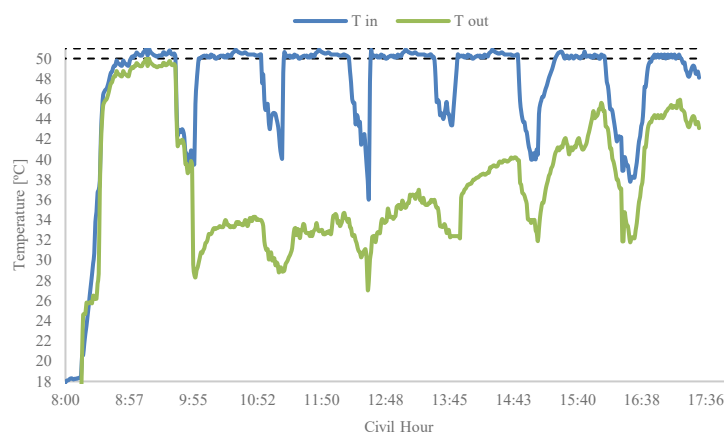


Figure 11. Drying temperature

Temperature control remained unchanged throughout the six tomato drying tests conducted throughout the four seasons, demonstrating both the stability of the process and the versatility of the indirect solar dehydrator. Furthermore, the quality of the product obtained has been well received in the local market in the city of Guanajuato, reflecting its acceptance and competitiveness compared to dehydrated products already on the market.

Drying efficiency

The drying efficiency is inversely proportional to the total amount of energy that falls on the dehydrator. Temperature control, depending on the solar energy captured and removed by the air, allows the amount of energy incident on the dehydrator to be regulated. Figure 12 shows the drying efficiency evaluated in each of the 6 drying tests during the year 2024. It can be observed that the test carried out on March 13th presented the highest drying efficiency of 58.2% (deep blue bar). 8.7 kg of free water was removed using 1.13 kW of energy to evaporate

it. The drying efficiency on March 14th decreased by up to 90% (light blue bar), since the amount of water evaporated was 0.89 kg, with the energy supplied to the solar device being 12.8 times greater than the energy required to evaporate the free water. 0.13 kW of energy was used to evaporate the free water on this second day. The average drying efficiency was 32.1% (black bar). The total energy incident on the solar dehydrator was 1.94 and 1.6 kW for March 13th and 14th.

The test conducted on February 7th showed an efficiency of 46.4% for the first day deep blue bar), while the second day saw a reduction of 90% (light blue bar). The average efficiency for the day was 25.55% (black bar), and the incident energy amounts were 1.9 and 2.4 kW for February 7th and 8th. The November 1st test showed the lowest efficiencies, with values of 22.3 and 2.0% for days 1 (deep blue bar) and 2 (light blue bar), respectively, with an average drying efficiency of 12.8% (black bar). The total incident energy on the solar dehydrator was 3.14 and 3.0 kW for November 1st and 2nd.

Despite the fluctuation in irradiance levels, it can be observed that the drying efficiency of the solar dehydrator is above those reported in the literature by Sharma *et al.* [20], Cetina *et al.* [21], and Chouikhi and Amer [22], who performed their tests in a temperature range between 31.4 and 54 °C and under irradiance conditions of 400 to 700 W/m².

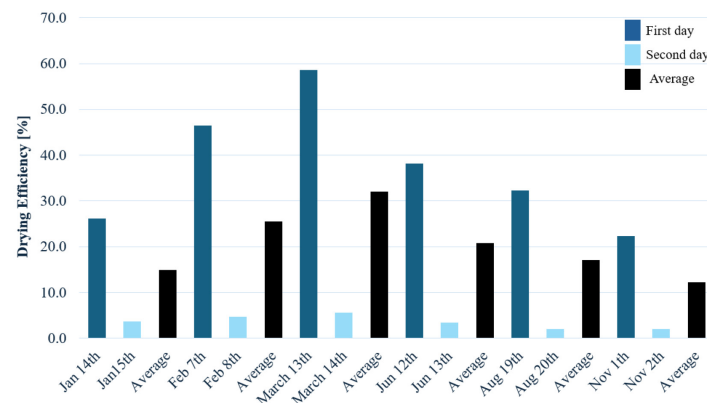


Figure 12. Drying efficiencies

CONCLUSIONS

Tomato dehydration research presented in this article differs from that previously published. It jointly quantifies the impact of environmental conditions using the graphical boxplot method. Drying kinetics is characterised using the results of the environmental conditions assessment to maximise drying efficiency and production by reducing drying times. To intensify moisture removal, tomato wedges were cut as flat plates, with moisture removal carried out on both sides of the wedge.

Drying time was reduced by 40% based on literature reports. The shortest drying time was 9.6 h for the March 13th test.

In drying kinetics, more than one environmental variable defines the speed of the process. It depends on a combination of environmental variables, which present maximums and minimums at different times of the year. June presented the highest irradiance levels (median, mean, and mode of 755, 734, and 938 W/m²). However, the relative humidity reported in this test increased by 8.8% compared to March 13th. Drying time increased by 26%.

The diffusion coefficient increased by 53% for the March 13th test. In all tests, drying efficiency was higher than that reported in the literature, with values of up to 58%.

Future work is to determine the relationship between dehydrated product and food safety by eliminating or reducing tomato losses.

ACKNOWLEDGMENTS

The authors wish to thank the Rector's Office of the Guanajuato Campus of the University of Guanajuato for the financial support provided for the modernisation of the meteorological station at Pueblito de Rocha Campus.

NOMENCLATURE

Symbols

a	Percentile 25th, 50 th , 75 th	
A	Solar collector area	[m ²]
D_{eff}	Effective diffusion coefficient	[m ² /s]
E	Thermal energy	[kJ]
E_{in}	Solar energy incident	[kJ]
F	Uncertainty	
G	Irradiance	[W/m ²]
HR	Relative humidity	[%]
m	Tomato mass	[g]
M	Moisture content	[g water/g dry solid]
N	Total number of data points	
Q	Quartile	
t	Time	[h] or [s]
Δt	Time increment	[h]
T	Drying temperature	[°C]
T_a	Ambient temperature	[°C]
V	Air speed	[m/s]
w	Uncertainty of each variable	
x	Independent variables for uncertainty	

Greek letters

λ	Latent heat
-----------	-------------

Subscripts and superscripts

c	Critical
d	Dry solid and drying
db	Dry basis
e	Equilibrium
evap	Evaporation
o	Initial
r	Radius
vap	Vapour
w	Water
wb	Wet basis

Abbreviations

SDG	Sustainable Development Goal
IQR	Interquartile range

REFERENCES

1. M. Y. Ali, A. A. I. Sina, S. S. Khandker, L. Neesa, E. M. Tanvir, A. Kabir, M. I. Khalil, and S. H. Gan, “Nutritional composition and bioactive compounds in tomatoes and their impact on human health and disease: A review”, *Foods*, vol. 10, no. 1, p. 1-32, Dec. 2020, <https://doi.org/10.3390/foods10010045>.
2. I. Domínguez, J. L. del Río, V. Ortiz-Somovilla, and E. Cantos-Villar, “Technological innovations for reducing tomato loss in the agri-food industry”, *Food Research International*, vol. 203, p. 1-11. Elsevier Ltd, Feb. 01, 2025, <https://doi.org/10.1016/j.foodres.2025.115798>.
3. F. and A. O. of the U. N. FAO, “Agricultural production statistics 2010–2023. FAOSTAT Analytical Briefs”, 2024, [Online]. Available: <https://www.fao.org/faostat/en/#data/QCL>, [Accessed Feb. 01, 2025].
4. M. Bath, T. Erickson, P. Xie, P. Miglani, and Y. Wang, “The Weight of Tomato Waste: A systemic approach to global food loss”, in *Proceedings of Relating Systems Thinking and Design RSD-13*, Oslo, Norway, 2024. [Online]. Available: <https://rsdsymposium.org/tomato-waste/> [Accessed Feb. 04, 2025].
5. Secretaría de Agricultura y Desarrollo Rural (SADER) (in Spanish, Ministry of Agriculture and Rural Development), “México, referente mundial en el cultivo y exportación de jitomate: Agricultura” (in Spanish, Mexico, a Global Benchmark in Tomato Cultivation and Export: Agriculture), 2022. [Online]. Available: <https://www.gob.mx/agricultura/prensa/mexico-referente-mundial-en-el-cultivo-y-exportacion-de-jitomate-agricultura>, [Accessed: Feb. 01, 2025].
6. World Bank, “Pérdidas y Desperdicios de Alimentos en México. Una Perspectiva Económica, Ambiental y Social” (in Spanish, Food Loss and Waste in Mexico: An Economic, Environmental, and Social Perspective), Washington, DC: The World Bank, 2017. Available: <https://documents1.worldbank.org/curated/en/099935205102329984/pdf/IDU0505d2b880c5bc040af0b30d01ba538edebc6.pdf>, [Accessed: Feb. 02, 2025].
7. T. Shamah-Levy, E. Lazcano-Ponce, L. Cuevas-Nasu, M. Romero-Martínez, E. Gaona-Pineda, L. Gómez-Acosta, L. Mendoza-Alvarado, and I. Méndez-Gómez-Humarán, “Encuesta Nacional de Salud y Nutrición Continua 2023. Resultados Nacionales” (in Spanish, 2023 Continuous National Health and Nutrition Survey: National Results), Cuernavaca, Mexico: Instituto Nacional de Salud Pública, 2024. Available: <https://insp.mx/novedades-editoriales/encuesta-nacional-de-salud-y-nutricion-continua-2023-resultados-nacionales>, [Accessed: Feb. 04, 2025].
8. N. Prabhu, D. Saravanan, and S. Kumarasamy, “Eco-friendly drying techniques: a comparison of solar, biomass, and hybrid dryers”, *Environ Sci Pollut Res Int*, vol. 30, no. 42, pp. 95086–95105, Sep. 2023, <https://doi.org/10.1007/s11356-023-28807-z>.
9. Z. Berk, “Dehydration”, in *Food Process Engineering and Technology*. New York, USA: Elsevier, 2018, chapter 22, pp. 459–510, <https://doi.org/10.1016/B978-0-12-373660-4.00022-3>.
10. R. Olmos-Cruz, “Modelo analítico de un deshidratador 100% solar” (in Spanish, Analytical Model of a 100% Solar Dehydrator), M. Eng. Thesis, University of Guanajuato, Guanajuato, 2024.
11. F. and A. O. of the U. N. FAO, “Trade Reforms and Food Security. Conceptualizing the Linkages”, 2003, [Online]. Available: <https://www.fao.org/4/y4671e/y4671e00.pdf>, [Accessed: Feb. 03, 2025].

12. A. Khalil, A. M. Khaira, R. H. Abu-Shanab, and M. Abdelgaied, “A comprehensive review of advanced hybrid technologies that improvement the performance of solar dryers: Photovoltaic/thermal panels, solar collectors, energy storage materials, biomass, and desalination units”, *Solar Energy*, vol. 253, Elsevier Ltd, pp. 154–174, Mar. 15, 2023, <https://doi.org/10.1016/j.solener.2023.02.032>.
13. G. Martínez-Rodríguez, “Scaling up to a pilot plant for a mobile solar dehydrator, for its technical-economic feasibility, with field products from Hidalgo and Bajío from Guanajuato” (in Spanish, Escalamiento a planta piloto de deshidratador solar móvil, para su factibilidad técnico-económica, con productos de campo de Hidalgo y del bajío de Guanajuato) (Technical) Report, CONACYT/316058, National Council of Science and Technology, Mexico city, Mexico, 2023.
14. Y. Yao, Y. X. Pang, S. Manickam, E. Lester, T. Wu, and C. H. Pang, “A review study on recent advances in solar drying: Mechanisms, challenges and perspectives”, *Solar Energy Materials and Solar Cells*, vol. 248, Elsevier B.V., pp. 1–20, Dec. 01, 2022, <https://doi.org/10.1016/j.solmat.2022.111979>.
15. T. A. Hamed and A. Alshare, “Environmental Impact of Solar and Wind energy-A Review”, *Journal of Sustainable Development of Energy, Water and Environment Systems*, vol. 10, no. 2, pp. 1–23, Jan. 2022, <https://doi.org/10.13044/j.sdewes.d9.0387>.
16. T. Ramírez, Y. Meas, D. Dannehl, I. Schuch, L. Miranda, T. Rocks, and U. Schmidt, “Water and carbon footprint improvement for dried tomato value chain”, *J Clean Prod*, vol. 104, pp. 98–108, Oct. 2015, <https://doi.org/10.1016/j.jclepro.2015.05.007>.
17. D. D. Behera, R. C. Mohanty, and A. M. Mohanty, “Performance Evaluation of Indirect Type Forced Convection Solar Mango Dryer. A Sustainable Way of Food Preservation”“, *Thermal Science*, vol. 27, no. 2, pp. 1659–1672, 2023, <https://doi.org/10.2298/TSCI220621154B>.
18. M. Sandali, A. Boubekri, and D. Mennouche, “Thermal and Economical Study of a Direct Solar Dryer with Integration of Different Techniques of Heat Supply”, in *Springer Proceedings in Energy*, A. Belasri and S. A. Beldjilali, Eds. Singapore, Malaysia: Springer Nature, 2020, ch. 73, pp. 585–595.
19. S. Suherman, R. Rilna, N. Afriandi, E. Susanto, and H. Hadiyanto, “Drying of tomato slices using solar drying method”, in *AIP Conf Proc*, Feb. 2023, vol. 2667, no. 1, <https://doi.org/10.1063/5.0112428>.
20. M. Sharma, D. Atheaya, and A. Kumar, “Performance evaluation of indirect type domestic hybrid solar dryer for tomato drying: Thermal, embodied, economical and quality analysis”, *Thermal Science and Engineering Progress*, vol. 42, Jul. 2023, <https://doi.org/10.1016/j.tsep.2023.101882>.
21. A. J. Cetina-Quñones, J. López López, L. Ricalde-Cab, A. El Mekaoui, L. San-Pedro, and A. Bassam, “Experimental evaluation of an indirect type solar dryer for agricultural use in rural communities: Relative humidity comparative study under winter season in tropical climate with sensible heat storage material”, *Solar Energy*, vol. 224, pp. 58–75, Aug. 2021, <https://doi.org/10.1016/j.solener.2021.05.040>.
22. H. Chouikhi and B. M. A. Amer, “Performance Evaluation of an Indirect-Mode Forced Convection Solar Dryer Equipped with a PV/T Air Collector for Drying Tomato Slices”, *Sustainability (Switzerland)*, vol. 15, no. 6, Mar. 2023, <https://doi.org/10.3390/su15065070>.
23. S. Tera, S. Sinon, M. Diakite, K. P. Mathos, and O. Sanogo, “Modelling of Indirect Solar Drying with and without a Thermal Storage Unit for Tomatoes”, *Engineering*, vol. 17, no. 04, pp. 259–275, 2025, <https://doi.org/10.4236/eng.2025.174016>.

24. Abuelnuor A. A., A. A. M. Omara, I. K. Salih, E. K. M. Ahmed, R. M. Babiker, and A. A. M. Mohammedali, "Experimental Study on Tomato Drying Using a Solar Dryer Integrated with Reflectors and Phase Change Material," *2020 International Conference on Computer, Control, Electrical, and Electronics Engineering (ICCCEEE)*, Khartoum, Sudan, 2021, pp. 1-5, <https://doi.org/10.1109/ICCCEEE49695.2021.9429617>.
25. A. Lingayat, V. P. Chandramohan, V. R. K. Raju, and A. Kumar, "Development of indirect type solar dryer and experiments for estimation of drying parameters of apple and watermelon: Indirect type solar dryer for drying apple and watermelon", *Thermal Science and Engineering Progress*, vol. 16, May 2020, <https://doi.org/10.1016/j.tsep.2020.100477>.
26. A. W. Noori, M. J. Royen, and J. Haydary, "An active indirect solar system for food products drying", *Acta Chimica Slovaca*, vol. 12, no. 1, pp. 142–149, Apr. 2019, <https://doi.org/10.2478/acs-2019-0020>.
27. M. B. Silva, "Avaliação de um secador solar em diferentes condições climáticas e meteorológicas (in Portuguese, Evaluation of a Solar Dryer Under Different Climatic and Weather Conditions)", *Research, Society and Development*, vol. 11, no. 1, p. e15411124405, Jan. 2022, <https://doi.org/10.33448/rsd-v11i1.24405>.
28. A. Benseddik, A. Azzi, F. Chellali, R. Khanniche, and K. Allaf, "An analysis of meteorological parameters influencing solar drying systems in Algeria using the isopleth chart technique", *Renew Energy*, vol. 122, pp. 173–183, Jul. 2018, <https://doi.org/10.1016/j.renene.2018.01.111>.
29. R. A. Olmos-Cruz, G. Martínez-Rodríguez, E. Sánchez-García, and J. C. Baltazar, "Analysis of Environmental Variables during Apple Dehydration", *Chem Eng Trans*, Dec. 2024, vol. 114, pp. 37–42, <https://doi.org/10.3303/CET24114007>.
30. R. L. Nuzzo, "The Box Plots Alternative for Visualizing Quantitative Data", *PM and R*, vol. 8, no. 3, pp. 268–272, Mar. 2016, <https://doi.org/10.1016/j.pmrj.2016.02.001>.
31. J. Ocon García and G. Tojo Barreiro, "Secado de Sólidos" (in English, Drying of Solids), in *Problemas de Ingeniería Química: operaciones básicas (in English, Chemical Engineering Problems: Basic Operations)*, Fifth ed., vol. 2. Madrid, Spain: Aguilar, 1980, ch. 9, pp. 240–323.
32. A. Lingayat, V. P. Chandramohan, and V. R. K. Raju, "Design, Development and Performance of Indirect Type Solar Dryer for Banana Drying", *Energy Procedia*, Mar. 2017, vol. 109, pp. 409–416, <https://doi.org/10.1016/j.egypro.2017.03.041>.
33. A. Djebli, S. Hanini, O. Badaoui, and M. Boumahdi, "A new approach to the thermodynamics study of drying tomatoes in mixed solar dryer", *Solar Energy*, vol. 193, pp. 164–174, Nov. 2019, <https://doi.org/10.1016/j.solener.2019.09.057>.
34. V. R. Mugi and V. P. Chandramohan, "Shrinkage, effective diffusion coefficient, surface transfer coefficients and their factors during solar drying of food products – A review", *Solar Energy*, vol. 229, pp. 84–101, Nov. 2021, <https://doi.org/10.1016/j.solener.2021.07.042>.
35. M. Fterich, M. Ibrahim Elamy, E. Touti, and H. Bentaher, "Experimental and numerical study of tomatoes drying kinetics using solar dryer equipped with PVT air collector", *Engineering Science and Technology, an International Journal*, vol. 47, pp. 1-13, Nov. 2023, <https://doi.org/10.1016/j.jestch.2023.101524>.
36. X. Xu, Y. Chen, B. Li, Z. Zhang, G. Qin, T. Chen, and S. Tian, "Molecular mechanisms underlying multi-level defense responses of horticultural crops to fungal pathogens", *Hortic Res*, vol. 9, 2022, pp. 1–13, <https://doi.org/10.1093/hr/uhac066>.
37. D. Ji, W. Liu, L. Jiang, and T. Chen, "Cuticles and postharvest life of tomato fruit: A rigid cover for aerial epidermis or a multifaceted guard of freshness?", *Food Chem*, vol. 15, no. 411, Jan. 2023, <https://doi.org/10.1016/j.foodchem.2023.135484>.
38. J. Crank, "Diffusion in a plane sheet", in *The Mathematics of Diffusion*, Second ed., London, U.K.: Oxford University Press, 1975, ch. 4, p. 44-69.

39. O. Badaoui, S. Hanini, A. Djebli, B. Haddad, and A. Benhamou, “Experimental and modelling study of tomato pomace waste drying in a new solar greenhouse: Evaluation of new drying models”, *Renew Energy*, vol. 133, pp. 144–155, Apr. 2019, <https://doi.org/10.1016/j.renene.2018.10.020>.
40. Instituto Nacional de Ecología y Cambio Climático (INECC) (in Spanish, National Institute of Ecology and Climate Change), “Factores De Emisión Para Los Diferentes Tipos De Combustibles Fósiles Y Alternativos Que Se Consumen En México (in Spanish, Emission Factors for the Different Types of Fossil and Alternative Fuels Consumed in Mexico)”, Coyoacán, Mexico, 2014. [Online]. Available: <http://www.inecc.gob.mx>. [Accessed: Feb. 10, 2025].
41. C. Nettari, A. Boubekri, A. Benseddik, S. Bouhoun, D. Daoud, A. Badji, and I. Hasrane, “Design and performance evaluation of an innovative medium-scale solar dryer with heat recovery based-latent heat storage: Experimental and mathematical analysis of tomato drying”, *J Energy Storage*, vol. 88, May 2024, <https://doi.org/10.1016/j.est.2024.111559>.
42. W. Mühlbauer and J. Müller, “Tomato (*Solanum lycopersicum* L.)”, in *Drying Atlas*, Elsevier, 2020, Chapter 6.3, pp. 195–205.



Paper submitted: 12.03.2025

Paper revised: 24.07.2025

Paper accepted: 24.07.2025